Diagn Interv Radiol 2023; DOI: 10.4274/dir.2023.221959

CHEST IMAGING

ORIGINAL ARTICLE

Photon-counting computed tomography in the assessment of rheumatoid arthritis-associated interstitial lung disease: an initial experience

Nikolett Marton
Janos Gyebnar
Kinga Fritsch
Judit Majnik
Gyorgy Nagy
Judit Simon
Veronika Müller
Adam Domonkos Tarnoki
David Laszlo Tarnoki
Pal Maurovich-Horvat

PURPOSE

Interstitial lung disease (ILD) accounts for a significant proportion of mortality and morbidity in patients with rheumatoid arthritis (RA). The aim of this cross-sectional study is to evaluate the performance of novel photon-counting detector computed tomography (PCD-CT) in the detection of pulmonary parenchymal involvement.

METHODS

Sixty-one patients with RA without a previous definitive diagnosis of ILD underwent high-resolution (HR) (0.4 mm slice thickness) and ultra-high-resolution (UHR) (0.2 mm slice thickness) PCD-CT examination. The extent of interstitial abnormalities [ground-glass opacity (GGO), reticulation, bronchiectasis, and honeycombing] were scored in each lobe using a Likert-type scale. Total ILD scores were calculated as the sum of scores from all lobes.

RESULTS

Reticulation and bronchiectasis scores were higher in the UHR measurements taken compared with the HR protocol [median (quartile 1, quartile 3): 2 (0, 3.5) vs. 0 (0, 3), $P < 0.001$ and 2 (0, 2) vs. 0 (0, 2), $P < 0.001$, respectively]; however, GGO and honeycombing scores did not differ [2 (2, 4) vs. 2 (2, 4), $P = 0.944$ and 0 (0, 0) vs. 0 (0, 0), $P = 0.641$, respectively]. Total ILD scores from both HR and UHR scans showed a mild negative correlation in diffusion capacity for carbon monoxide (HR: r = –0.297, $P = 0.034$; UHR: r = –0.294, $P = 0.036$). The pattern of lung parenchymal involvement did not differ significantly between the two protocols. The HR protocol had significantly lower volume CT dose index [0.67 (0.69, 1.06) mGy], total dose length product [29 (24.48, 33.2) mGy*cm] compared with UHR scans [8.18 (6.80, 9.23) mGy, $P < 0.001$ and 250 (218, 305) mGy*cm, $P < 0.001$].

CONCLUSION

UHR PCD-CT provides more detailed information on ILD in patients with RA than low-dose HR PCD-CT. HR PCD-CT image acquisition with a low effective radiation dose may serve as a valuable, low-radiation screening tool in the selection of patients for further, higher-dose UHR PCD-CT screening.

KEYWORDS

CT, high-resolution, low-dose, lung, photon-counting, ultra-high-resolution

From the Department of Radiology (N.M., J.G., J.S., A.D.T., D.L.T., P.M-H. ✉ maurovich-horvat.pal@semmelweis.hu), Medical Imaging Centre, Semmelweis University, Budapest, Hungary; Department of Rheumatology (K.F., J.M., G.N.), Buda Hospital of the Hospitaller Order of Saint John of God, Budapest, Hungary; Department of Rheumatology and Clinical Immunology (J.M., G.N.), Semmelweis University, Budapest, Hungary; MTA-SE Cardiovascular Imaging Research Group (J.S., P.M-H.), Semmelweis University, Budapest, Hungary; Department of Pulmonology (V.M.), Semmelweis University, Budapest, Hungary; Department of Oncologic Imaging and Invasive Diagnostic Radiology (A.D.T., D.L.T.), National Institute of Oncology, Budapest, Hungary.

Received 25 October 2022; revision requested 16 November 2022; last revision received 05 January 2023; accepted 22 January 2023.

Epub: 08.03.2023

Publication date: 29.03.2023

DOI: 10.4274/dir.2023.221959

Contrary to conventionally utilized energy-integrating detectors (EIDs), photon-counting detectors (PCDs) are able to directly convert X-ray photons into electric pulses.[1] This process leads to better spatial resolution, decreased beam hardening, reduced noise and radiation dose, and to register the energy of photons.[2-4] PCD-computed tomography (PCD-CT) has gained increasing interest in pulmonary imaging due to its high spatial resolution.[5] To date, preclinical studies have mostly investigated lung PCD-CT imaging by analyzing optimal reconstruction parameters, such as matrix size, optimal slice thickness, and iterative reconstruction algorithms.[6,7]

You may cite this article as: Marton N, Gyebnar J, Fritsch K, et al. Photon-counting computed tomography in the assessment of rheumatoid arthritis-associated interstitial lung disease: an initial experience. *Diagn Interv Radiol.* 2023;29(2):291-299.

Rheumatoid arthritis (RA) is a systemic autoimmune disease associated with several pathologies, including parenchymal and pleural involvement, bronchiolitis, rheumatoid nodules, and vascular abnormalities. Interstitial lung abnormalities (ILA) occur in 1.8%–67% of patients with RA, among whom established interstitial lung disease (ILD) accounts for a significant proportion of mortality and morbidity.[8,9] High-resolution (HR) CT remains the main imaging modality for the evaluation of lung involvement in RA.[10] The spectrum of RA-related interstitial abnormalities in parenchymal involvement includes ground-glass opacity (GGO), fibroreticular changes, bronchiectasis, and honeycombing. The most frequent phenotype of RA-ILD is usual interstitial pneumonitis (UIP).[11] It has been demonstrated that the early identification of subclinical ILAs (which show a tendency to progress to ILD) by CT promotes early intervention that stabilizes further interstitial changes and, thus, significantly improves prognosis.[12]

The primary goal of this study is to evaluate the performance of PCD-CT in the detection of early and subclinical parenchymal lung involvement in patients with RA.

Methods

Patients

From February 2022 to November 2022, 334 patients were enrolled in this study (Figure 1). Inclusion criteria were as follows: (i) patients diagnosed with RA (according to 2010 American College of Rheumatology/European League Against Rheumatism classification criteria); and (ii) patients >40 years of age. Exclusion criteria were as follows: (i) patients with pulmonary infection, lung malignancies, or previously diagnosed ILD. The demographic data, clinical manifestations, and routine laboratory test results of study participants were recorded. All patients were checked regularly and received medical treatment as recommended by the attending rheumatologist, following standards of care. First second of forced expiration, forced vital capacity, and diffusion capacity for carbon monoxide (DLCO) were measured by pulmonologists via pulmonary function tests. Patients underwent yearly chest X-rays following their RA diagnosis; however, based on earlier radiographs, none had an HR CT-based indication to rule out ILD. Written informed consent was obtained from all study participants. Three hundred twenty-six patients underwent HR CT imaging, and, following the detection of abnormalities by the attending radiologist, 61 patients underwent a subsequent ultra-high resolution (UHR) CT on the same day for further evaluation of lung parenchyma (Figure 1).

Main points

- Cross-sectional study shows that ultra-high-resolution (UHR) photon-counting detector computed tomography (PCD-CT) imaging provides more detailed information regarding interstitial lung disease (ILD) in patients with rheumatoid arthritis (RA) than HR PCD-CT.
- PCD-CT might be a promising tool in the early diagnosis of subclinical ILD and bronchiectasis in patients with RA.
- Low-dose, HR PCD-CT could serve as a means of preselecting candidates for more detailed, UHR measurements in the assessment of RA-related ILD.

Research ethics

This trial was registered on the clinicaltrials.gov website (IV-2683-1/2022/EKU) and approved by the local ethical review board (2021, National Scientific and Research Ethics Committee, Hungary). This work was carried out in accordance with the Helsinki Declaration (JAMA 2000; 284:3043–3049).[13]

Patient PCD-CT measurements

HR (slice thickness: 0.4 mm) and UHR (slice thickness: 0.2 mm) CT scans were carried out with a PCD-CT scanner (Naeotom Alpha®, Siemens Healthineers, Erlangen, Germany). Both imaging techniques were performed with a large field of view (FOV) [median (quartile 1, quartile 3): 35 (32, 38) cm] and 1024 × 1024 matrix. Additionally, quantitative iterative reconstruction algorithms were utilized to enhance image quality (Table 2). To exclude GGO from dependent atelectasis, prone inspiratory HR CT measurements were performed.

Phantom studies

To compare the image quality of PCD- and EID-CT methods, prone chest region measurements with matched parameters (similar slice thicknesses and equivalent rotation times, voltage and current, pitch values, and scan lengths) were taken of a

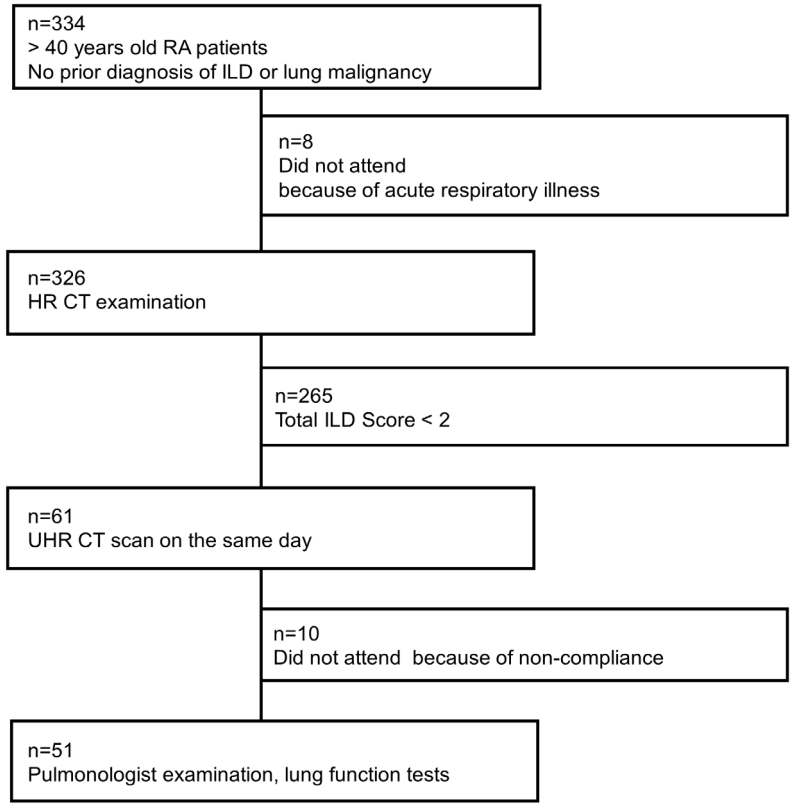

Figure 1. Flow chart of study sample and processing. Patients with rheumatoid arthritis who were <40 years of age, had pneumonia in the previous 3 months, or suffered from an already diagnosed interstitial lung disease or lung tumor were excluded. After the first low-dose, high-resolution (HR) chest computed tomography (CT) scan, radiologist specialists scored interstitial lung abnormalities (ground-glass opacity, reticulation, bronchiectasis, and honeycombing) based on a Likert-type scale. If these were absent or very low (scores <2), no ultra-high-resolution (UHR) measurement was conducted (n = 265), resulting in our final cohort with both HR and UHR CT (n = 61). RA, rheumatoid arthritis; ILD, interstitial lung disease.

phantom (CT Whole Body Phantom, PBU-60) with a 1-year-old PCD-CT scanner (Naeotom Alpha®, Siemens Healthineers, Erlangen, Germany), a 2.5-year-old 128-slice EID-CT scanner (Philips Incisive®, Philips, Amsterdam, The Netherlands), and a 2-year-old 128-slice EID-CT scanner (GE Revolution EVO®, GE Healthcare, Chicago, Illinois, USA). Subjective image quality was rated independently by four radiologists on a five-point scale (5 being best, 1 being worst). Contrast-to-noise ratio (CNR) was calculated based on the formula: [average pixel values in signal region of interest (ROI) (bronchial wall) – average pixel values of background ROI (air)] / standard deviation (SD) of background ROI (air). Signal-to-noise ratio (SNR) was calculated based on the formula: average pixel values in signal ROI (bronchial wall)/SD of background ROI (air).

Dose values

Volume CT dose index (CTDIvol) and total dose length product (TDLP) values were extracted from patient protocol data (syngo. via software, Siemens Healthineers). Approximate effective dose values were calculated from TDLP values as follows: Effective dose = TDLP × *k*-factor (0.014 mSv/mGy*cm).[14,15]

Evaluation of parenchymal abnormalities

All PCD-CT images were reviewed, and specific ILD patterns were determined by consensus, by two radiologists with 6 and 13 years of experience. A third thoracic radiologist with 13 years of experience then reviewed the images and spoke with the ILD board to reach an agreement with the pulmonologists. Interstitial abnormalities were classified into four categories: GGO (parenchymal opacity with perceptible underlying bronchovascular structure without architectural distortion), reticulation (thickening of interlobular septae or intralobular septae and traction), bronchiectasis (dilatation of bronchial tree), and honeycombing (clustered, subpleural, multilayered, cystic air-spaces).

To test whether the UHR protocol provided additional information about interstitial pathologies, a semiquantitative scoring system was utilized. The extent of pulmonary parenchymal abnormalities for each lobe was scored using a Likert-type scale (0 = absent; 1 = 1%–25%; 2 = 26%–50%; 3 = 51%–75%; 4 = 76%–100%). Total GGO, reticulation, bronchiectasis, and honeycombing scores were calculated by adding up the scores of all five lung lobes, with final values ranging from 0–20. All scores were combined to produce a total ILD HR CT score ranging from 0–80 (Figure 2).[16,17]

As ILD is a heterogeneous group of parenchymal lung disorders, observed abnormalities were classified into patterns defined in Table 3.

Statistical analysis

Distribution was defined by the Kolmogorov–Smirnov test. Descriptive statistics (median and quartiles) and mean ± SD were used to represent abnormally and normally distributed variables, respectively. A paired t-test was used to compare normally distributed data, and the Wilcoxon test was used to compare non-parametric data. In the case of parenchymal changes with a definitive ILD pattern, Cohen's kappa (κ) was used to test agreement between readers (0–0.20 = poor agreement; 0.21–0.40 = fair agreement; 0.41–0.60 = moderate agreement; 0.61–0.80 = substantial agreement; and 0.81–1.00 = almost perfect agreement).[18] The Pearson correlation coefficient was used to find correlations between total lung HR CT scores and pulmonary function tests. Differences between the image quality parameters of different CTs were evaluated using a One-Way ANOVA test with a subsequent Tukey post-hoc analysis. Significance was established at *P* values <0.05 were considered statistically significant. Categorical variables were reported as frequencies and percentages. Statistical analyses were performed using GraphPad Prism v. 6.0 software.

Results

Demographic and clinical characteristics

Of the 334 patients initially enrolled, eight were excluded due to the presence of an acute lung infection, and 265 were excluded due to the absence of significant interstitial changes in the initial HR CT scan (total ILD score <2) (detailed descriptions in the section entitled: assessment of parenchymal abnormalities). Sixty-one patients underwent

a

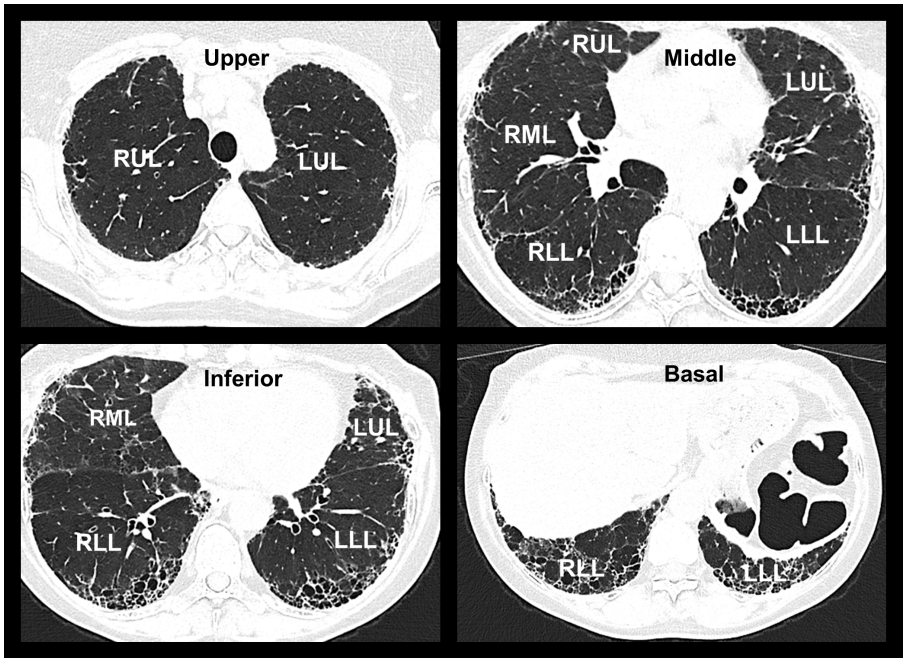

b

	RUL	RML	RLL	LUL	LLL	*Total*
GGO	0	0	0	0	0	*0*
Reticulation	1	1	1	1	1	*5*
Bronchiectasis	0	0	1	0	1	*2*
Honeycombing	1	1	3	2	3	*10*
Total ILD Score	**17**					

Figure 2. Four UHR CT images of a 68-year-old woman with RA at upper- and mid-level, inferior, and basal costophrenic angles revealed honeycombing, peripheral diffuse reticulation, and traction bronchiectasis with lower-zone dominance consistent with the pattern of definitive usual interstitial pneumonia **(a)**. Lung HR CT score was calculated based on Wangkaew et al.[20] **(b).** RUL, right upper lobe; RML, right middle lobe; RLL, right lower lobe; LUL, left upper lobe; LLL, left lower lobe; RA, rheumatoid arthritis; ILD, interstitial lung disease; UHR, ultra-high-resolution; HR, high-resolution; CT, computed tomography; GGO, ground-glass opacity.

Table 1. Patient characteristics and pulmonary function test results

Patient characteristics (n = 61, both HR and UHR scans)	
Gender [n (%)]	40 (65.60%) females; 21 (34.40%) males
Age (y) (mean ± SD)	68.6 ± 9.73
Time since disease onset (y) (mean ± SD)	15.75 ± 12.85
Rheumatoid factor positivity [n (%)]	42 (68.85%)
Anti-citrullinated protein antibody positivity [n (%)]	36 (59.01%)
Smoking history (ever-smokers) [n (%)]	33 (54.10%)
Pack-year among smokers (mean ± SD)	23.66 ± 20.40
Body mass index (kg/m^2) (mean ± SD)	27.4 ± 3.96
Previous COVID-19 pneumonia (not in the prior 3 months) [n (%)]	6 (9.83%)
Cough [n (%)]	16 (26.22%)
Dyspnea [n (%)]	18 (29.50%)
Fatigue [n (%)]	26 (42.62%)
Pulmonary function tests (n = 51)	
FVC (%) (mean ± SD)	90 ± 17.89
FEV1 (%) (mean ± SD)	93.23 ± 14.30
FEV1/FVC (%) (mean ± SD)	101.39 ± 9.66
DLCO (%) (mean ± SD)	108.39 ± 19.61

Age, duration from disease onset, smoking history, and body mass index are expressed as mean ± standard deviation. The proportion of seropositivity, smokers, and clinical symptoms are presented as percentages. COVID-19, coronavirus disease 2019; DLCO, diffusion capacity for carbon monoxide; FEV1, first second of forced expiration; FVC, forced vital capacity; HR, high-resolution; ILD, interstitial lung disease; SD, standard deviation; UHR, ultra-high-resolution.

both HR and UHR scans, and 51 patients underwent pulmonary function tests (Table 1). The mean age of study participants was 68.6 ± 9.73 years, and 40 (65.57%) were female. Average time since disease onset was 15.75 ± 12.85 years. Forty-two (68.85%) patients were seropositive, and 33 (53.22%) had previously been smokers. The detailed characteristics of the study population are summarized in Table 1.

Assessment of parenchymal abnormalities

Parenchymal abnormalities were visually recognizable on both HR and UHR scans (Figure 3). UHR CTs yielded higher total ILD scores than HR CTs [6 (4, 9) vs. 4 (2.5, 8), $P < 0.001$). Additionally, bronchiectasis and reticulation scores were significantly higher in the UHR protocol compared with the HR protocol [2 (0, 2) vs. 0 (0, 2), $P < 0.001$ and 2 (0, 3.5) vs. 0 (0, 3) $P < 0.001$, respectively]; however, GGO and honeycombing scores did not differ [2 (2, 4) vs. 2 (2, 4), $P = 0.944$ and 0 (0, 0) vs. 0 (0, 0), $P = 0.641$, respectively] (Figure 4). Visually identified patterns did not differ significantly between UHR and HR PCD-CT protocols (Figure 5). UIP patterns, non-specific interstitial pneumonia, desquamative interstitial pneumonia, respiratory bronchiolitis-ILD, pleuroparenchymal fibroelastosis, and post-coronavirus disease-2019 parenchymal changes were registered in the examined population on both HR and UHR protocols (Figure 5). No patterns of lymphocytic interstitial pneumonitis or organizing pneumonia were identified on the scans. Inter-reader reliability pattern scores varied between moderate and perfect agreement (Figure 5). Most cases were small-extent, otherwise non-specified parenchymal ab-

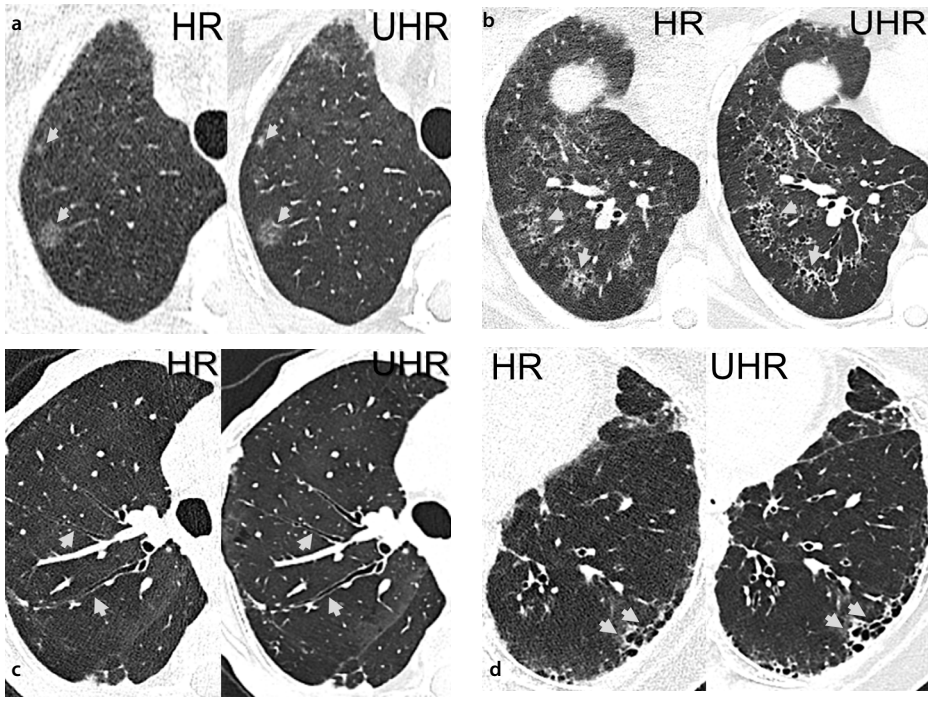

Figure 3. Non-contrast HR (left) and UHR (right) chest photon-counting detector. CT scans at the same level represent interstitial abnormalities (indicated by gray arrows): upper-zone GGO **(a)**, middle-zone peribronchovascular fibrosis **(b)**, middle-zone bronchiectasis **(c)**, and lower-zone honeycombing **(d)**. Images are derived from four different RA patients with different patterns of parenchymal involvement: respiratory bronchiolitis interstitial lung disease (ILD) **(a)**; desquamative interstitial pneumonia-ILD **(b)**; non-specified ILA **(c)**; and dUIP **(d)**. UHR, ultra-high-resolution; HR, high-resolution; CT, computed tomography; GGO, ground-glass opacity; RA, rheumatoid arthritis; ILA, interstitial lung abnormalities; dUIP, definitive usual interstitial pneumonia.

normalities. Total ILD scores of both HR and UHR protocols showed a mild but significant negative correlation with DLCO values (HR: r = –0.297, P = 0.034; UHR: r = –0.294; P = 0.036) (Figure 6).

Dose considerations and phantom studies

Reduced-dose, 0.4 mm scans had significantly lower CTDIvol values [median (quartile 1, quartile 3): 0.67 (0.69, 1.06) mGy] compared with non-reduced, 0.2 mm scans [8.18 (6.80, 9.23) mGy, P < 0.001]. The 0.4 mm slice thickness HR acquisitions had approximately 8.6 × lower TDLP [29.0 (24.48, 33.20) mGy*cm] compared with 0.2 mm slice thickness, non-reduced-dose UHR scans [250 (218, 305) mGy*cm, P < 0.001]. Median effective radiation doses were ~0.4 mSv for low-dose (LD) HR CT scans and 3 mSv for UHR CT scans (Table 2). Dose-matched phantom studies confirmed that, compared with EID-CT scans, PCD-CT measurements had improved subjective and objective image quality values (Figure 7).

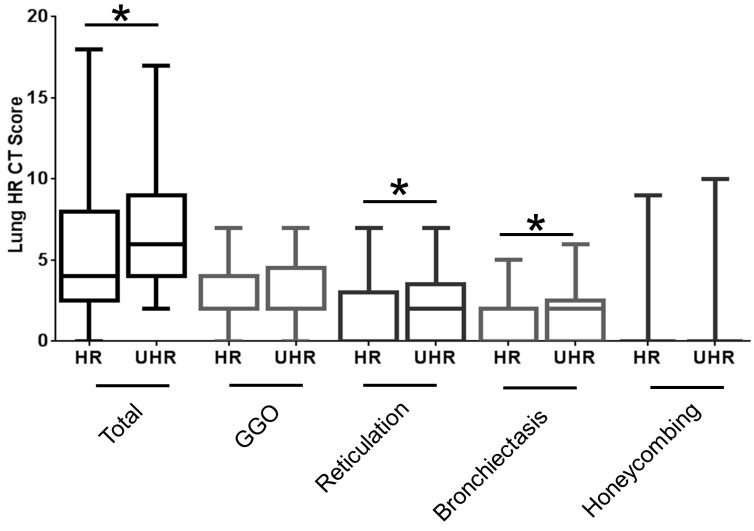

Figure 4. Box and whiskers diagram of interstitial lung disease scores.[17] GGO, reticulation, bronchiectasis, and honeycombing values represent scores from all the five lobes. Total scores were calculated from the sum of GGO, reticulation, bronchiectasis, and honeycombing values. UHR measurements had slightly higher total, reticulation, and bronchiectasis scores. Inner horizontal lines indicate median values. Whiskers represent minimum to maximum range. Results were considered statistically significant at P < 0.05 (asterisk marks). GGO, ground-glass opacity; UHR, ultra-high-resolution; HR, high-resolution; CT, computed tomography.

Discussion

A relatively small number of studies on the clinical application of PCD-CT in lung diseases have been published. This current work extends previous observations. This study demonstrates that LD PCD-CT chest scans could be used to evaluate the quality and extent of ILA in a majority of patients with RA, and higher-accuracy UHR imaging can add further information about lung parenchymal involvement. Thus, HR PCD-CT with a low effective radiation dose may serve as a valuable screening tool in the selection of RA-ILD patients for a more detailed, higher-dose UHR PCD-CT screening.

RA is a systemic autoimmune disease, and lung involvement may be its most frequent extra-articular manifestation and highest contributor to a worsening prognosis.[19] The prevalence of interstitial lung involvement is reported in a wide spectrum of patients with RA, and ILD can be a predictor of the development of articular manifestations.[9,20,21] Some forms of ILD are progressive, and, in addition to their patterns, the ILD board considers the extent of lung involvement an important parameter in its multidisciplinary discussion.[22,23] Screening for ILD may be advisable in select cases of RA, as early detection of parenchymal changes could help direct antirheumatic treatment.[24]

The identification of interstitial lung involvement requires high spatial resolution scans, as the subtlety of parenchymal changes (e.g., intralobular reticulations, bronchiectasis, and honeycombing) are frequently

a

Total number of examined patients n=61	**Radiologist 1,2 (number of diagnosed patterns)**			**Radiologist 3 (number of diagnosed patterns)**			**Interobserver agreement (Cohen's Kappa)**	
Pattern	HR	UHR	p	HR	UHR	p	HR	UHR
dUIP	8	8	(HR vs.	8	8	(HR vs.	1	1
pUIP	4	4	UHR)	3	4	UHR)	0.65	1
iUIP	1	0	0.97	0	0	1	0.65	1
NSIP	3	3	(ns)	5	5	(ns)	0.73	0.73
OP	0	0		0	0		1	1
LIP	0	0		0	0		1	1
RB-ILD	2	1		3	2		0.79	0.65
DIP	0	1		0	1		1	1
PPFE	2	1		2	1		1	1
postCOVID	2	2		2	2		1	1
otherwise non-specified	41	41		38	38		0.89	0.89

b

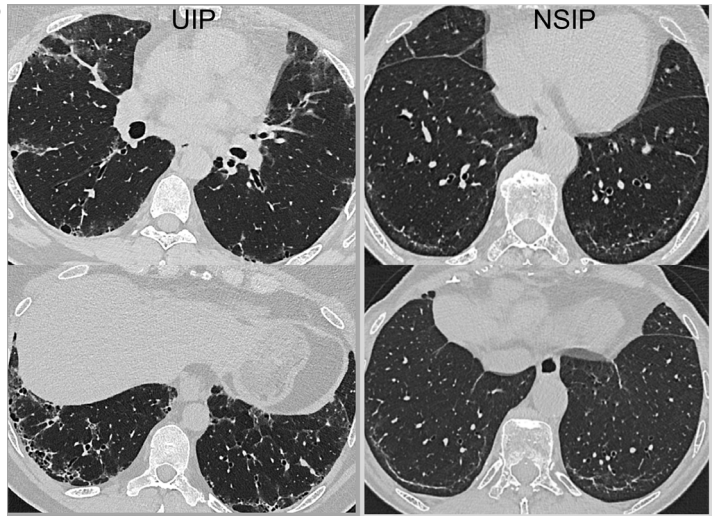

Figure 5. Patterns of ILD identified **(a)** in the examined RA population (n = 61). Axial 0.2 mm slice thickness chest PCD-CT images representing the most common ILD patterns patients with RA **(b)** usual interstitial pneumonitis (left), non-specific interstitial pneumonia (right). ILD, interstitial lung disease; PCD-CT, photon-counting detector-computed tomography; RA, rheumatoid arthritis; UHR, ultra-high-resolution; HR, high-resolution; dUIP, definitive usual interstitial pneumonia; pUIP, probable usual interstitial pneumonia; iUIP, indeterminate usual interstitial pneumonia; OP, organizing pneumonia; LIP, lymphocytic interstitial pneumonia; DIP, desquamative interstitial pneumonia; PPFE, pleuro-parenchymal fibroelastosis; COVID, coronavirus, NSIP, non-specific interstitial pneumonia; ns, non-significant.

indefinite.[25] To date, there is no worldwide consensus on screening recommendations because the benefits of lung parenchymal involvement screening have had to be balanced with the inherent risks of ionizing radiation. Large FOV chest PCD-CT scans with 1024 × 1024 matrix sizes conferred better overall image quality and SNR than standard EID-CT scans.[6,26] According to previous studies, LD image acquisition with PCD-CT showed better SNR and attenuation accuracy compared with conventional CT, especially at lower doses, where attenuation decreased significantly with EID-CT.[7] Better image quality was also observed, especially in areas with known beam hardening (e.g., paravertebral spaces). Prior investigations have shown that PCD-CT images have 15.2%–16.8% less noise at two different dose levels. Furthermore, studies have proven that HR parameters could be preserved while applying LD protocols in lung evaluation.[26] In this examination, fast gantry rotation times (0.25–0.5 s) were used to reduce scanning time and motion artifacts.[27] We used a 1024 × 1024 matrix, large FOV (35 ± 3 cm, depending on the size of the patient), and 0.2 or 0.4 mm slice thickness parameter protocols and found a satisfactory detection of parenchymal pathologies, including GGOs, fibrotic reticulations, bronchiectasis, and subpleural cysts (Table 2, Figure 4). According to the literature, lower tube currents are optimal for pulmonary nodule detection (approximately 25 mA).[28] However, for subtle parenchymal anomalies, higher currents are inevitable to reach better resolutions. In the case of this study, 100 kV (for HR) and 120 kV (for UHR) voltages, as well as automated mA parameters, were utilized to obtain a HR image with reduced dose values (Table 2).

Optimized dose efficiency, combined with iterative reconstruction algorithms, can decrease noise levels and allow for large matrix reconstructions that lead to ultra-LD protocols.[29,30] Due to increased data complexity and spectral information, a novel algorithm, quantum iterative reconstruction, with four strength levels (QIR-1–4) has been developed for PCD-CT.[29] According to a preceding article, QIR-3 dispensed the highest spatial resolution and noise texture; thus, we applied QIR-3 for our protocols.[29] Additionally, it has been described that significant dose reduction and conservation of HR parameters for lung parenchyma assessment is possible with PCD-CT, either with or without iterative reconstruction.

In a pilot study, Inoue et al.[31] demonstrated that PCD-CT produced better image qual-

a

	FVC(%)	FEV1(%)	FEV1/FVC(%)	DLCO(%)
HR CT	r=0.029, p=0.083	r=0.076, p=0.596	r=0.128, p=0.371	r=-0.297, *p=0.034
UHR CT	r=-0.016, p=0.910	r=0.090, p=0.529	r=0.180, p=0.449	r=-0.294, *p=0.036

b

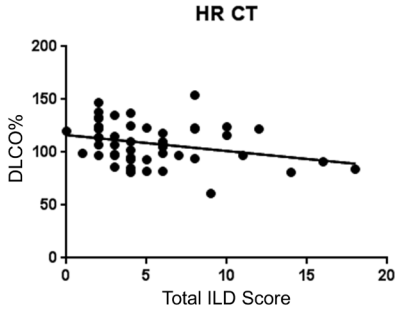

c

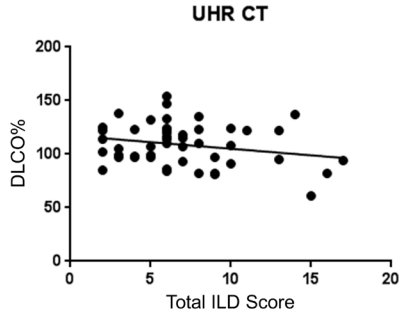

Figure 6. Correlation values of pulmonary function tests and total ILD scores **(a)**. Both HR **(b)** and UHR **(c)** total ILD scores show a mild, significant negative correlation with DLCO values (%). *, $P < 0.05$; UHR, ultra-high-resolution; HR, high-resolution; CT, computed tomography; FVC, forced vital capacity; FEV1, first second of forced expiration; DLCO, diffusion capacity for carbon monoxide; ILD, interstitial lung disease.

Table 2. RA patient PCD-CT chest protocol characteristics

	HR	UHR
Rotation time (s)	0.25	0.5
Collimation	144 × 0.4	120 × 0.2
Pitch	1.5	0.85
kV	100	120
Filter	Standard	Standard
mA based on size (automated) (mean ± SD)	96 ± 25.2	86 ± 21.6
Total mAs based on size (automated) (mean ± SD)	217 ± 75.6	194.36 ± 64.8
Quantitative iterative reconstruction algorithm/strength	3	3
Matrix size	1024 × 1024	1024 × 1024
Kernel	Bl60	Bl60
Slice thickness (mm)	0.4	0.2
Slice increment (mm)	0.4	0.2
Pixel size (mm)	FOV/matrix size	FOV/matrix size
Care keV IQ level	15	100

LD, low dose; HR scan and sequential UHR scan was carried out without the administration of contrast media. HR, high-resolution; UHR, ultra-high-resolution; SD, standard deviation; RA, rheumatoid arthritis; PCD-CT, photon-counting detector computed tomography; BL, body lung kernel; FOV, field of view.

a

	PCD_A	PCD_B	EID1_A	EID1_B	EID2_A	EID2_E
Slice thickness (mm)	0.6	1	0.67	1	0.625	1
Rotation time (s)	0.5	0.5	0.5	0.5	0.5	0.5
Nominal single collimation	0.2	0.2	0.625	0.625	0.625	0.625
Pitch	1	1	1	1	1	1
kV	100	100	100	100	100	100
mA	100	100	100	100	100	100
Matrix size	512x512	512x512	512x512	521x512	512x512	521x51
Kernel	Bl60	Bl60	Lung	Lung	Lung	Lung
Scan length (cm)	31.00	31.00	32.00	32.00	32.00	32.00
Scan time (s)	2.3	2.6	6	6.5	8.5	8.8
TDLP (mGy*cm)	29.40	29.50	187	187	70.7	101
CTDIvol	0.83	0.84	4.84	4.83	2.98	2.98
Subjective Score (median [Q1;Q3])	4 [4;4]	4 [4.5;5]	2.5 [2;3]	3 [2;3]	4 [3;4]	4 [4;4]
Subjective Score/ TDLP	**0.14***	**0.16***	0.01	0.02	0.06	0.04
Subj Score Median/ CTDI	**4.82***	**5.35***	0.51	0.62	1.34	1.34
SNR	6.06	7.38	1.02	1.72	5.69	1.15
CNR	21.93	29.11	19.98	38.47	26.60	33.87
SNR/TDLP	**0.20***	**0.25***	0.01	0.01	0.08	0.01
SNR/CTDI	**7.30***	**8.79***	0.21	0.36	1.91	0.38
CNR/TDLP	**0.74***	**0.98***	0.11	0.21	0.08	0.06
CNR/CTDI	**26.43***	**34.65***	4.13	7.96	1.91	0.38

b

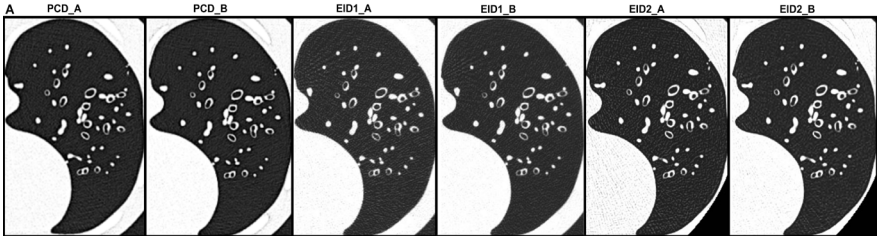

Figure 7. Matched-parameter scan protocols, dose values, and image quality parameters of different PCD and energy-integrating detector (EID) scans **(a)**. Axial images of identical inferior chest regions **(b)** PCD-CT images have proven ($P < 0.05$) dose-matched subjective and objective image quality compared with EID-CT images. *, $P < 0.05$; PCD-CT, photon-counting detector-computed tomography; CTDIvol, volume CT dose index; TDLP, total dose length product; CNR, contrast-to-noise-ratio; SNR, signal-to-noise ratio; BL, body lung kernel.

ity and enhanced diagnostic confidence for lung parenchymal abnormalities at reduced radiation doses. Jungblut et al.[32] further confirmed that PCD-CT provides good image quality with lower radiation doses, compared with EID-CT. Our phantom studies confirmed that, compared with EID-CT measurements, PCD-CT protocols produce improved dose-matched CNR and SNR values (Figure 7). Previous LD EID-CT protocols (i.e., <1 mSv) are not recommended for diagnostic use, as their impaired image quality could lead to the misclassification of ILD.[33] Chest HR EID-CT has an effective dose of approximately 6–9 mSv, according to the literature, while in our study, the effective dose of PCD-CT was 0.4 mSv for HR scans and 3.5 mSv for UHR scans. Previously reported average LD EID-CT protocols had an effective dose of 2.1–2.4 mSv, significantly higher than our HR PCD-CT dose value.[13,26,32,34] LD CT has been increasingly used in the assessment of pulmonary cancer; however, this is not the only pulmonary disorder in which the risk–benefit ratio could be positive. For instance, the follow-up of ILD at low doses of radiation could be of interest.[33,35,36,37,38] Our data suggest that PCD-CT is a promising tool in radiation dose optimization, which is crucial in optimizing the risk–benefit ratio of CT lung screening.[39]

UHR scans proved to be more sensitive in the detection of bronchiectasis and reticulation; hence, their total score values were slightly higher. However, the identification of GGO and honeycombing values was the same between protocols (Figure 4). The UHR protocol was slightly more sensitive to interstitial pathologies; however, the magnitude of differences was not protruding. Moreover, the same ILD patterns were identified with both protocols. Taking into consideration the dose values that were notably lower (~7.4×) in LD HR scans, the LD measurements were able to assess interstitial changes with good proximity.

While this study has limitations (e.g., the relatively low number of patients enrolled), it is comparable to other international investigations. Furthermore, it would be interesting to set against our results from other PCD-CT protocols with different parameters. However, the benefits of better image quality need to be balanced with the risks of higher radiation exposure in these patients. Phantom studies to compare different detector-type CT protocols can be conducted to avoid increased radiation doses for patients. Additionally, ILD multidisciplinary team discussions are needed to gauge the difference between these two CT modalities in clinical settings to improve team diagnosis, especially of early cases. Longitudinal radiological data on natural behavior and disease-specific treatment of early RA-ILD are also needed.

In conclusion, wide-scale clinical experience with UHR CT imaging to assess lung involvement in patients with RA does not exist. In this proof-of-concept study, we found that a UHR PCD-CT protocol provided more detailed images compared with an HR PCD-CT protocol. The HR PCD-CT protocol provided detailed information regarding interstitial lung involvement; however, in the case of an extended or complex pathology, additional UHR imaging may prove beneficial. Further studies are needed to determine if an HR PCD-CT protocol, with its reduced radiation doses, could serve as an initial screening tool before selecting patients for further UHR imaging. From a clinical perspective, the higher effective radiation dose of UHR PCD-CT is balanced by its better characterization of pulmonary involvement, which provides the potential for earlier anti-fibrotic treatment, a very important intervention in RA patients with ILD.

Table 3. Patterns of interstitial lung involvement

Pattern name	Main characteristics (based on HR CT)
Definitive usual interstitial pneumonia	Honeycombing, +/– traction bronchiectasis, reticular abnormalities, distribution: subpleural, basal dominant; absence of features suggestive of an alternative diagnosis.
Probable usual interstitial pneumonia	Reticulations, +/– superimposed GGO, peripheral traction bronchiectasis/bronchiolectasis, distribution: subpleural, basal dominant; absence of features suggestive of an alternative diagnosis.
Indeterminate usual interstitial pneumonia	Subtle reticular abnormalities, +/– superimposed GGO, distribution: does not suggest different pathology.
Non-specific interstitial pneumonia	GGOs with basal predominance and subpleural sparing, subpleural reticulations, thickening of bronchovascular bundles in fibrotic type, traction bronchiectasis, distribution: subpleural, symmetrical, apicobasal gradient.
Organizing pneumonia	Patchy consolidation with a predominantly subpleural and/or peribronchial distribution, peribronchial or peribronchiolar nodules, thickened interlobular septae, bronchial wall thickening, GGO or crazy paving.
Desquamative interstitial pneumonia	Bilateral symmetric GGO, mostly basal and peripheral, irregular linear opacities, small cystic spaces (occasional).
Respiratory bronchiolitis interstitial lung disease	Slight upper-zone predilection of GGOs, poorly defined centrilobular nodules, smoking-related changes.
Pleuro-parenchymal fibroelastosis	Bilateral apical pleural thickening, architectural distortion, reticular abnormalities, peripheral consolidation, traction bronchiectasis, pneumothorax (occasional).
Lymphocytic interstitial pneumonia	Diffuse to mid- and lower-zone dominance, peribronchovascular thickening, reticulation, subpleural or centrilobular nodules, GGOs, scattered, thin-walled cysts.
Otherwise non-classifiable pattern	None of the above and/or cannot be characterized due to small extent (≤5%).

Interstitial lung disease is a heterogeneous group of chronic parenchymal diseases. The specific patterns listed belong to the ILD category. GGO, ground glass opacity[10]; HR, high-resolution; CT, computed tomography; ILD, interstitial lung disease.

Acknowledgements

We would like to thank for the help and support of the colleagues mentioned afterwords:

Hanna Balogh MD[1], Leila Szeibel MD[1], Tamas Purczel MD[1], Tamas Munkacsi MD[1], Nora Kerkovits MD[1], Klaudia Borbely MD[1], Laszlo Szakacs[1], Aniko Kubovje[1], Kinga Karlinger MD, PhD[1], Dora Sarvari MD[2], Timea Petri MD[2]

[1]Department of Radiology, Medical Imaging Centre, Semmelweis University, Budapest, Hungary

[2]Buda Hospital of the Hospitaller Order of Saint John of God, Budapest, Hungary

Conflict of interest disclosure

The authors declared no conflicts of interest.

Funding

Nikolett Marton MD, PhD (first author) received a Bolyai Research Scholarship from the Hungarian Academy of Sciences.

References

1. Taguchi K, Iwanczyk JS. Vision 20/20: single photon counting x-ray detectors in medical imaging. *Med Phys*. 2013;40(10):100901. [CrossRef]
2. Willemink MJ, Persson M, Pourmorteza A, Pelc NJ, Fleischmann D. Photon-counting CT: technical principles and clinical prospects. *Radiology*. 2018;289(2):293-312. [CrossRef]
3. Danielsson M, Persson M, Sjölin M. Photon-counting X-ray detectors for CT. *Phys Med Biol*. 2021;66(3):03TR01. [CrossRef]
4. Rajendran K, Petersilka M, Henning A, et al. First clinical photon-counting detector CT system: technical evaluation. *Radiology*. 2022;303(1):130-138. [CrossRef]
5. Ferda J, Vendiš T, Flohr T, et al. Computed tomography with a full FOV photon-counting detector in a clinical setting, the first experience. *Eur J Radiol*. 2021;137:109614. [CrossRef]
6. Hata A, Yanagawa M, Honda O, et al. Effect of matrix size on the image quality of ultra-high-resolution CT of the lung: comparison of 512×512, 1024×1024, and 2048×2048. *Acad Radiol*. 2018;25(7):869-876. [CrossRef]
7. Symons R, Pourmorteza A, Sandfort V, et al. Feasibility of dose-reduced chest CT with photon-counting detectors: initial results in humans. *Radiology*. 2017;285(3):980-989. [CrossRef]
8. Jacob J, Hirani N, van Moorsel CHM, et al. Predicting outcomes in rheumatoid arthritis related interstitial lung disease. *Eur Respir J*. 2019;53(1):1800869. [CrossRef]
9. Fazeli MS, Khaychuk V, Wittstock K, et al. Rheumatoid arthritis-associated interstitial lung disease: epidemiology, risk/prognostic factors, and treatment landscape. *Clin Exp Rheumatol*. 2021;39(5):1108-1118. [CrossRef]
10. Raghu G, Remy-Jardin M, Richeldi L, et al. Idiopathic pulmonary fibrosis (an update) and progressive pulmonary fibrosis in adults: an official ATS/ERS/JRS/ALAT clinical practice guideline. *Am J Respir Crit Care Med*. 2022;205(9):18-47. [CrossRef]
11. Spagnolo P, Lee JS, Sverzellati N, Rossi G, Cottin V. The lung in rheumatoid arthritis: focus on interstitial lung disease. *Arthritis Rheumatol*. 2018;70(10):1544-1554. [CrossRef]
12. Juge PA, Crestani B, Dieudé P. Recent advances in rheumatoid arthritis-associated interstitial lung disease. *Curr Opin Pulm Med*. 2020;26(5):477-486. [CrossRef]
13. No authors listed. World Medical Association Declaration of Helsinki: ethical principles for medical research involving human subjects. *JAMA*. 2000;284(23):3043-3045. [CrossRef]
14. Smith-Bindman R, Lipson J, Marcus R, et al. Radiation dose associated with common computed tomography examinations and the associated lifetime attributable risk of cancer. *Arch Intern Med*. 2009;169(22):2078-2086.

[CrossRef]

15. Larke FJ, Kruger RL, Cagnon CH, et al. Estimated radiation dose associated with low-dose chest CT of average-size participants in the National Lung Screening Trial. *AJR Am J Roentgenol*. 2011;197(5):1165-1169. [CrossRef]
16. Kazerooni EA, Martinez FJ, Flint A, et al. Thin-section CT obtained at 10-mm increments versus limited three-level thin-section CT for idiopathic pulmonary fibrosis: correlation with pathologic scoring. *AJR Am J Roentgenol*. 1997;169(4):977-983. [CrossRef]
17. Wangkaew S, Euathrongchit J, Wattanawittawas P, Kasitanon N. Correlation of delta high-resolution computed tomography (HRCT) score with delta clinical variables in early systemic sclerosis (SSc) patients. *Quant Imaging Med Surg*. 2016;6(4):381-390. [CrossRef]
18. McHugh ML. Interrater reliability: the kappa statistic. *Biochem Med (Zagreb)*. 2012;22(3):276-282.
19. Turesson C. Extra-articular rheumatoid arthritis. *Curr Opin Rheumatol*. 2013;25(3):360-366. [CrossRef]
20. Mori S, Cho I, Koga Y, Sugimoto M. Comparison of pulmonary abnormalities on high-resolution computed tomography in patients with early versus longstanding rheumatoid arthritis. *J Rheumatol*. 2008;35(8):1513-1521. [CrossRef]
21. Turesson C, O'Fallon WM, Crowson CS, Gabriel SE, Matteson EL. Occurrence of extraarticular disease manifestations is associated with excess mortality in a community based cohort of patients with rheumatoid arthritis. *J Rheumatol*. 2002;29(1):62-67. [CrossRef]
22. Robles-Perez A, Luburich P, Rodriguez-Sanchon B, et al. Preclinical lung disease in early rheumatoid arthritis. *Chron Respir Dis*. 2016;13(1):75-81. [CrossRef]
23. American Thoracic Society; European Respiratory Society. American Thoracic Society/European Respiratory Society International Multidisciplinary Consensus Classification of the Idiopathic Interstitial Pneumonias. This joint statement of the American Thoracic Society (ATS), and the European Respiratory Society (ERS) was adopted by the ATS board of directors, June 2001 and by the ERS Executive Committee, June 2001. *Am J Respir Crit Care Med*. 2002;165(2):277-304. [CrossRef]
24. Picchianti Diamanti A, Markovic M, Argento G, et al. Therapeutic management of patients with rheumatoid arthritis and associated interstitial lung disease: case report and literature review. *Ther Adv Respir Dis*. 2017;11(1):64-72. [CrossRef]
25. Watadani T, Sakai F, Johkoh T, et al. Interobserver variability in the CT assessment of honeycombing in the lungs. *Radiology*. 2013;266(3):936-944. [CrossRef]
26. Bartlett DJ, Koo CW, Bartholmai BJ, et al. High-resolution chest computed tomography imaging of the lungs: impact of 1024 matrix reconstruction and photon-counting detector computed tomography. *Invest Radiol*. 2019;54(3):129-137. [CrossRef]
27. Mohamed SS, Ness DB, Sigovan M, et al. Review of an initial experience with an experimental spectral photon-counting computed tomography system. *Nucl Inst Methods Phys Res*. 2017;873:27-35. [CrossRef]
28. Beeres M, Wichmann JL, Paul J, et al. CT chest and gantry rotation time: does the rotation time influence image quality? *Acta Radiol*. 2015;56(8):950-954. [CrossRef]
29. Oguchi K, Sone S, Kiyono K, et al. Optimal tube current for lung cancer screening with low-dose spiral CT. *Acta Radiol*. 2000;41(4):352-356. [CrossRef]
30. Sartoretti T, Racine D, Mergen V, et al. Quantum iterative reconstruction for low-dose ultra-high-resolution photon-counting detector CT of the lung. *Diagnostics (Basel)*. 2022;12(2)522. [CrossRef]
31. Inoue A, Johnson TF, Voss BA, et al. A pilot study to estimate the impact of high matrix image reconstruction on chest computed tomography. *J Clin Imaging Sci*. 2021;11:52. [CrossRef]
32. Jungblut L, Euler A, von Spiczak J, et al. Potential of photon-counting detector CT for radiation dose reduction for the assessment of interstitial lung disease in patients with systemic sclerosis. *Invest Radiol*. 2022;57(12):773-779. [CrossRef]
33. Raghu G, Remy-Jardin M, Myers JL, et al. Diagnosis of idiopathic pulmonary fibrosis. An official ATS/ERS/JRS/ALAT clinical practice guideline. *Am J Respir Crit Care Med*. 2018;198(5):44-68. [CrossRef]
34. Sartoretti T, Landsmann A, Nakhostin D, et al. Quantum iterative reconstruction for abdominal photon-counting detector CT improves image quality. *Radiology*. 2022;303(2):339-348. [CrossRef]
35. Demb J, Chu P, Yu S,et al. Analysis of computed tomography radiation doses used for lung cancer screening scans. *JAMA Intern Med*. 2019;179(12):1650-1657. [CrossRef]
36. Ataç GK, Parmaksız A, İnal T, et al. Patient doses from CT examinations in Turkey. *Diagn Interv Radiol*. 2015;21(5):428-434. [CrossRef]
37. Molinari F, Tack DM, Boiselle P, et al. Radiation dose management in thoracic CT: an international survey. *Diagn Interv Radiol*. 2013;19(3):201-209. [CrossRef]
38. Topçuoğlu OM, Sarıkaya B. Fast kilovoltage-switching dual-energy CT offering lower x-ray dose than single-energy CT for the chest: a quantitative and qualitative comparison study of the two methods of acquisition. *Diagn Interv Radiol*. 2019;25(3):204-209. [CrossRef]
39. National Lung Screening Trial Research Team; Aberle DR, Berg CD et al. The National Lung Screening Trial: overview and study design. *Radiology*. 2011;258(1):243-253. [CrossRef]